

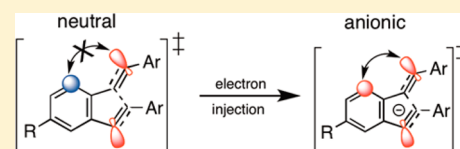
Orbital Crossings Activated through Electron Injection: Opening Communication between Orthogonal Orbitals in Anionic C1–C5 Cyclizations of Eneidyne

Paul W. Peterson, Nikolay Shevchenko, Boris Breiner, Mariappan Manoharan, Forat Lufti, Jess Delaune, Margaret Kingsley, Kirill Kovnir,[†] and Igor V. Alabugin*[‡]

Department of Chemistry and Biochemistry, Florida State University, 95 Chieftain Way, Tallahassee, Florida 32301, United States

S Supporting Information

ABSTRACT: Generally, the long-range electronic communication between spatially orthogonal orbitals is inefficient and limited to field and inductive effects. In this work, we provide experimental evidence that such communication can be achieved via intramolecular electron transfer between two degenerate and mutually orthogonal frontier molecular orbitals (MOs) at the transition state. Interaction between orthogonal orbitals is amplified when the energy gap between these orbitals approaches zero, or at an “orbital crossing”. The crossing between two empty or two fully occupied MOs, which do not lead to stabilization, can be “activated” when one of the empty MOs is populated (i.e., electron injection) or one of the filled MOs is depopulated (i.e., hole injection). In reductive cycloaromatization reactions, such crossings define transition states with energies defined by *both* the in-plane and out-of-plane π -systems. Herein, we provide experimental evidence for the utility of this concept using orbital crossings in reductive C1–C5 cycloaromatization reactions of eneidyne. Communication with remote substituents via orbital crossings greatly enhances regioselectivity of the ring closure step in comparison to the analogous radical cyclizations. We also present photophysical data pertaining to the efficiency of electron injection into the benzannelated eneidyne.



INTRODUCTION

The usual paradigm for using electronic effects in organic chemistry is based on the notion that efficient orbital overlap is needed to transmit conjugation¹ and hyperconjugation.² For example, the importance of orbital overlap is the conceptual foundation for the concept of stereoelectronic effects.³ Although this paradigm served well many generations of chemists and will continue to apply to the majority of organic reactions, it cannot help to control those reactions where such overlap is missing. A textbook example for the interruption of electronic communication imposed by spatial orthogonality is provided by steric inhibition of resonance (Figure 1). For example, once the acceptor nitro group is rotated so its π -system is orthogonal to the aromatic π -system of nitrobenzene, the accelerating effect of the acceptor on nucleophilic aromatic substitution is greatly diminished.⁴

C1–C6 Cyclizations of Eneidyne as a Probe of Remote Substituents. A less known but conceptually analogous example of poor communication between orthogonal π -systems is provided by the inefficiency of remote substituent effects in the Bergman cyclization⁵ of benzannelated eneidyne. Because remote substituents attached to the out-of-plane aromatic π -system cannot transmit electronic effects to the developing σ -radicals created from the orthogonal (in-plane) π -system,⁶ the rate of this reaction is insensitive to the substituent effects (Figure 2).^{7,8} This limitation has practical consequences because the Bergman cyclization and related cycloaromatization reactions⁹ find applications in the design of antitumor agents,¹⁰

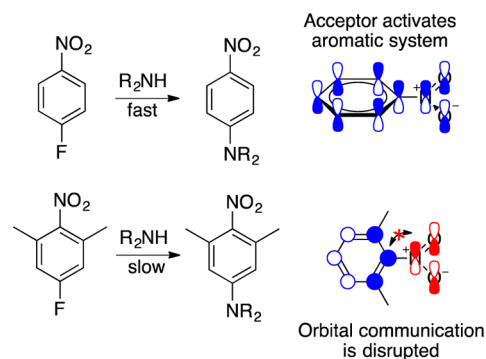


Figure 1. Steric inhibition of resonance: interruption of electronic communication imposed by spatial orthogonality.

sequence-specific DNA cleavers,¹¹ synthesis of polycyclic compounds,¹² and preparation of polymeric materials.¹³ The same limitation in the substituent control applies every time when a reaction involves breaking of a σ - or a π -bond in the presence of an orthogonal π -system (e.g., C–X bond scission in vinyl or aryl halides, other neutral cycloaromatization reactions, etc.).

Earlier, we provided computational evidence that analogous substituent effects become surprisingly large upon one-electron reduction of the eneidyne (Figure 2).¹⁴ This unusual trend suggested a new approach for overcoming inefficiency of orbital

Received: August 15, 2016

Published: November 6, 2016

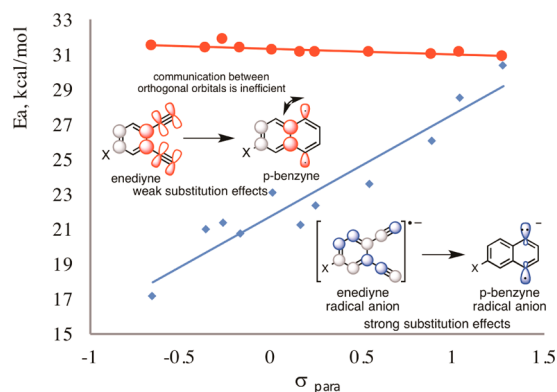


Figure 2. Inefficiency of substituent effects in the Bergman cyclizations of the benzannulated enediynes originates from orthogonality of the developing radical centers and the aromatic π -system. In contrast, the same remote substituents have pronounced effect on the activation energies of radical-anionic Bergman cyclization UBLYP/6-31G** barriers vs Hammett σ constants).

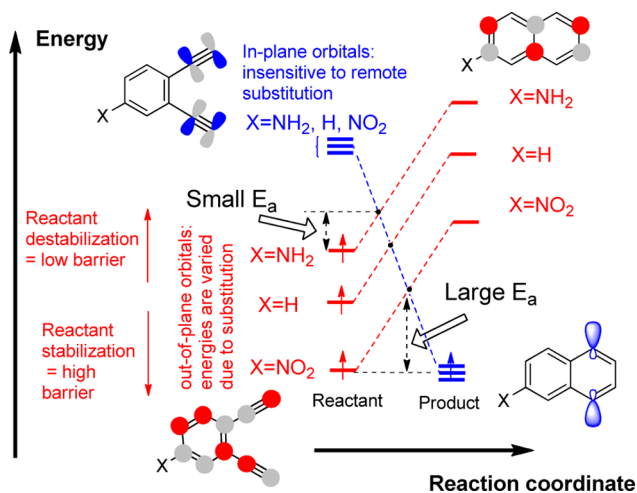


Figure 3. MO energy changes in the radical anionic Bergman cyclization. Changes in the out-of-plane enediyne MO energies are independent of changes in the in-plane enediyne MOs. The possibility of independent manipulation of MO energies allows one to control the relative energy needed to reach the crossing point between the two MO sets by either stabilization or destabilization of one of the sets while the other set is kept constant. Electron donors raise the out-of-plane MO energies (reactant destabilization). Electron acceptors decrease the out-of-plane MO energies (reactant stabilization).

control in cycloaromatization processes where transition-state (TS) energies are determined by *both* the out-of-plane and the in-plane molecular orbitals (MOs) coupled via intramolecular electron transfer (Figure 3). This approach allows one to manipulate the TS energies efficiently by utilizing reactant stabilization/destabilization as a way to control the activation barrier. The conceptual advantage of this approach is in its ability to fine-tune the relative energies of the two “non-interacting” MO sets in a rational way.¹⁵

In this approach, even negligible orbital interactions are sufficiently amplified when the energy gap between the interacting orbitals approaches zero (or when orbitals and the electronic states¹⁶ corresponding to the different population of these orbitals “cross”). This behavior follows from the known inverse dependence¹⁷ of the orbital interaction energy, ΔE_{stab} , between the energy gap between the interacting orbitals ΔE_{A-B} (Figure 4).

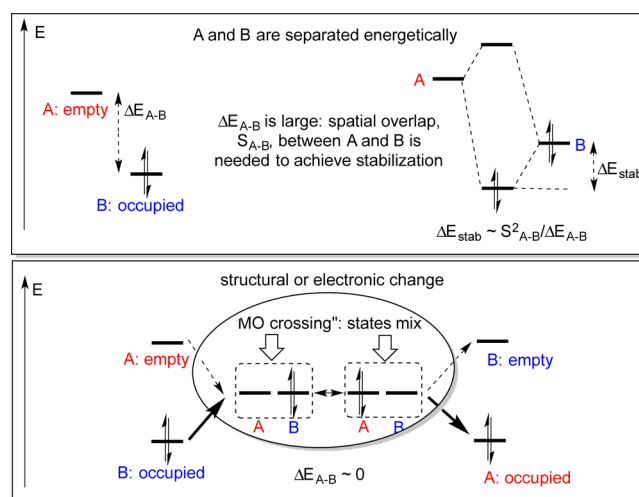


Figure 4. Amplification of orbital interactions by decreasing energy gap between the interacting orbitals. Orbital crossings allow intramolecular electron transfer between the orthogonal orbitals A and B.

The role of the energy gap on the interaction energies is well-documented.¹⁸ For example, it provides the basis of the common HOMO–LUMO approximation for the description of organic reactivity.

As the energy gap between the two interacting orbital approaches zero, the orbital mixing pattern changes from second to first order, and even small orbital overlap can be converted into a significant electronic interaction (Figure 4, bottom). In reductive cycloaromatization reactions, the electronic communication at the MO crossing enables electron transfer between the orthogonal π -systems. Because the crossing from the reactant to product electronic states involves an out-of-plane MO and in-plane MO, the TS energy is sensitive to both orthogonal π -arrays (*vide infra*).

Creating an Orthogonal MO Crossing. Two conditions are necessary for creating an MO crossing: (1) one MO should significantly change its energy and (2) the second MO should either stay at the same energy level or move *toward* the first MO (i.e., a higher energy MO moves up as a lower energy MO moves down). These conditions are satisfied if a bond is either broken or distorted in the presence of an orthogonal π -system.¹⁹ In particular, cycloaromatization reactions provide a very convenient tool for the study of MO crossings because these reactions always include two orthogonal π -systems, one of which directly participates in the formation of new bonds whereas the other remains an apparent bystander.²⁰ This situation creates two crossings that typically correspond to the HOMO/HOMO–1 crossing in the occupied manifold and LUMO/LUMO+1 crossing in the virtual orbitals.

This situation is illustrated in Figure 5. As a direct result of the bond-forming interaction, the in-plane π -orbitals are transformed into a σ -bond and a pair of nonbonding MOs (two radical centers). Consequently, the highest occupied in-plane MO (HOMO–1) at the TS is destabilized to the extent where it becomes the new HOMO. On the other hand, the respective unoccupied in-plane MO (LUMO+1) is *stabilized* and becomes the LUMO in the TS. In other words, the reactant HOMO and LUMO correspond to out-of-plane orbitals whereas, at the shorter C1–C6 or C1–C5 distances, the frontier MOs are localized at orthogonal (in-plane) nonbonding (radical) orbitals.

Because MOs in the top crossing in Figure 5 left are populated with zero electrons whereas MOs in the bottom crossing

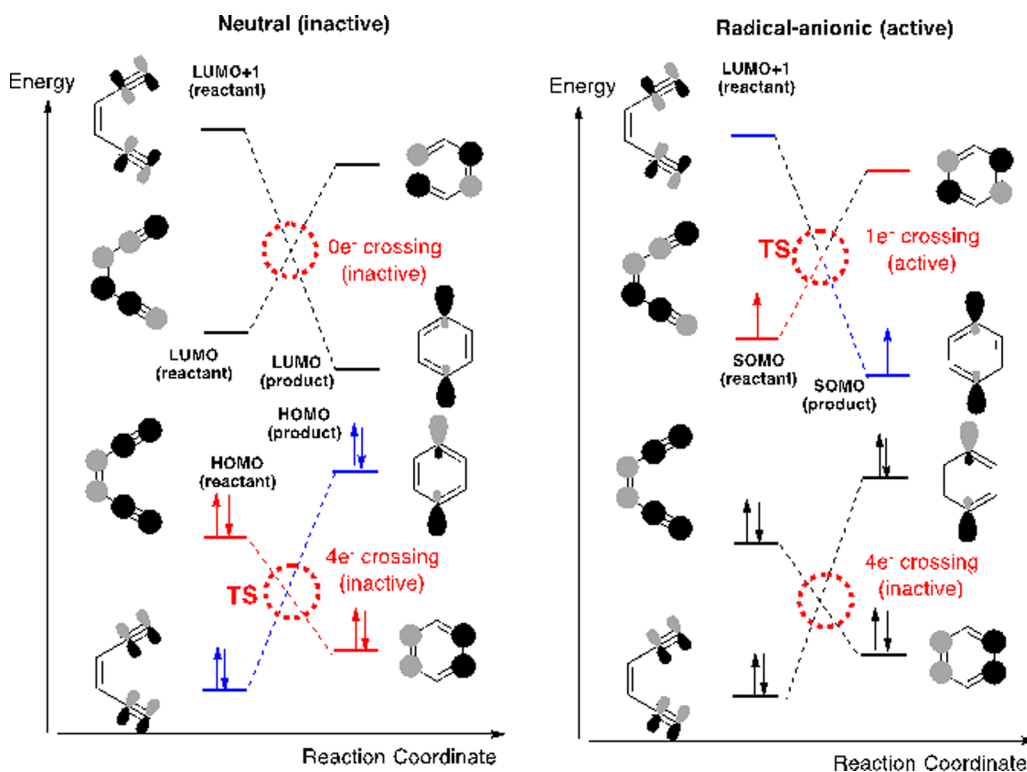


Figure 5. Crossings of in-plane and out-of-plane frontier MOs in neutral and radical-anionic Bergman cyclizations (similar crossings for photochemical, dianionic, and radical-cationic cyclizations involve the same MOs but differ in the number of electrons).

have four electrons, these MO crossings have little importance in the *thermal* Bergman cyclization. Interactions between two orbitals which are either fully filled or completely empty do not lead to stabilization.

Role of Electron Injection. Only once the donor orbital is at least partially filled (with either one or two electrons) and/or once the acceptor orbital is at least partially empty (either zero or one electrons), the stabilization is possible, as illustrated in the simplest case by 1e,2c, 2e,2c, and 3e,2c bonding patterns in Figure 6. Note that each of these patterns is directly accessible in cycloaromatization reactions if either an electron or a hole is “injected”. In particular, the top crossing in Figure 5 (left) can be activated by electron reduction, whereas the bottom crossing

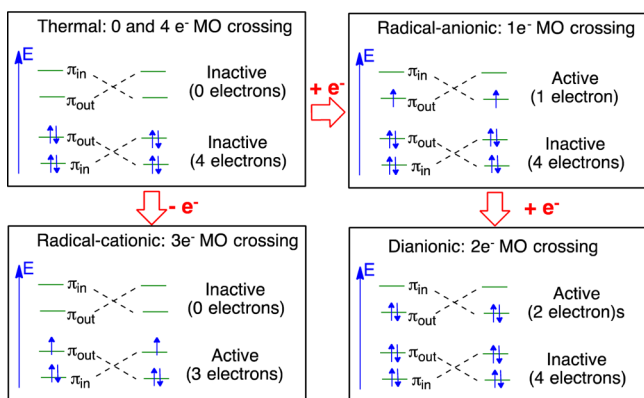


Figure 6. Difference in the number of electrons involved in the MO crossings activated by reduction or oxidation of a molecule containing orthogonal π -arrays. Labels “in” and “out” correspond to the in-plane and out-of-plane MOs. Note also that photochemical excitation (not shown here) will activate both 1e and 3e (hole) crossings.

in Figure 5 (right) can be activated via oxidation. The reductive MO crossings are likely to be important in the σ -C–Hal bond scission in the radical anions of aromatic halides, a process that starts to find a number of elegant synthetic applications.²¹

Vanishing HOMO–LUMO Gap, or When “Forbidden Reactions” Are Not Really Forbidden. As we discuss above, a MO crossing has to involve an empty and a filled orbital in order to influence chemical reactivity. In this situation, the HOMO–LUMO energy gap approaches zero. Engineering such situation in a closed shell molecule in its ground state is difficult, even though many applications in molecular electronics aim at minimizing this parameter. Furthermore, the “symmetry forbidden”²² scenario where the reactant HOMO correlates with the product LUMO and vice versa, imposes additional electronic penalty on the activation barrier.

However, when such crossings are activated either via an electron or a hole injection, the situation is different and the energy penalty due to the “forbiddenness” is minor. For example, the LUMO–SOMO²³ gap in the radical anions (Figure 5, Figure 7) is significantly lower than the HOMO–LUMO gap in the neutral molecules and, thus, no substantial additional barrier is imposed by the crossings. As the results, the anionic cycloaromatizations are “forbidden” only in a formal sense without a substantial energy penalty associated with the MO crossing.

In summary, the one-electron reduction of enediyne to the corresponding radical-anion populates the *out-of-plane* LUMO of the enediyne moiety. At the TS (the crossing), the electron is “transferred” between the orthogonal π -systems to the new (*in-plane*) LUMO. Moreover, analysis of electron density changes along the reaction path found that the activation barrier for both C1–C6 and C1–C5 cyclizations of enediyne radical-anions can be described as the avoided crossing between states corresponding to the population of the *out-of-plane* and *in-plane* MOs.¹⁴

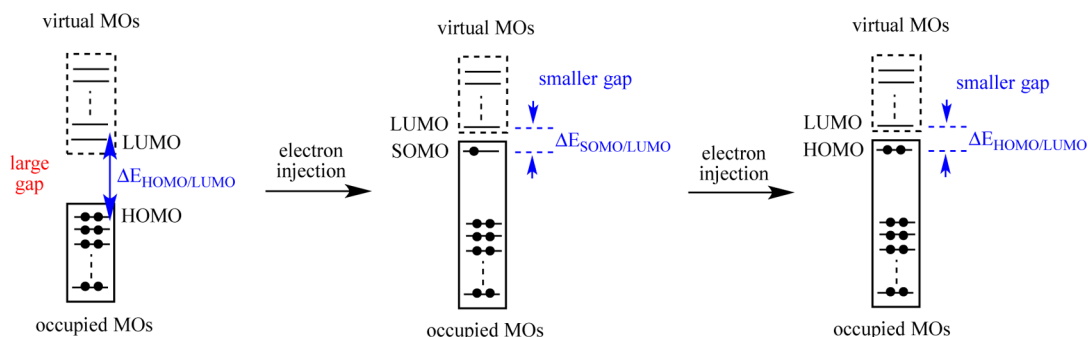


Figure 7. Changes in the HOMO–LUMO (and SOMO–LUMO) gaps due to the injection of one and two electrons in a typical molecule with a substantial ground-state HOMO–LUMO. Hole injection (one-electron oxidation) will also lead to a molecule with a low gap between SOMO (corresponding to the HOMO in the neutral reactant) and the next occupied MO (HOMO–1 in the neutral reactant). For simplicity, the effect of charge injection on MO energies is neglected.

As long as the electron population of the two crossing MOs is different, *even small electronic coupling between the two MOs will lead to communication between the orthogonal orbitals.* Such crossings do not affect thermal reactions whether the participating MOs are either empty or completely occupied because neither zero- nor four-electron interactions are stabilizing. However, both reduction and oxidation can activate the effect. This work reports experiments aimed to determine the relative efficiency of such *electronic control through 1e- and 2e-MO crossings.*

C1–C5 Cyclizations of Eneidyne as a Probe of Remote Substituent Effects. Although such MO crossings are general and should occur in a range of processes where either a σ - or a π -bond is broken in the vicinity of an orthogonal π -system in the TS where a structural change could lead to crossings of in-plane and out-of-plane MOs, we will concentrate on reductive C1–C5 cyclizations of eneidyne.

There are several reasons for the choice of C1–C5 cyclization as a model reaction. Our previous theoretical studies unraveled the combination of factors that renders the C1–C5 cyclization more favorable than the Bergman (C1–C6) pathway. Although the thermal version of this process is difficult,²⁴ this cyclization can be carried out either via a classic chemical reduction with lithium naphthalenide (Whitlock and co-workers)²⁵ for eneidyne with terminal Ph substituents or via photoinduced electron transfer (PET) for activated eneidyne with acceptor tetrafluoropyridinyl (TFP) substituents.²⁶ In the latter case, the reaction cascade continues toward the formation of more reduced (indene) products via an additional PET step.

The photoreductive C1–C5 cyclization is also interesting from a practical perspective. Most importantly, the overall eneidyne \rightarrow indene transformation corresponds to the formal transfer of four “H atoms” from the environment—twice that of the Bergman cyclization. We have shown that ratio of double-strand (ds) to single-strand (ss) DNA cleavage by bis-TFP eneidyne/lysine conjugates^{27,28} rivals that of natural antibiotic calicheamicin²⁹ whereas the analogous bis-lysine conjugates provide even greater ds:ss ratios.³⁰ We established that PET is indeed involved in the mechanism of DNA photo-damage³¹ and that it is possible to direct such DNA-cleavers toward the damaged DNA site, thus amplifying the damage and converting it into double stranded cleavage.³² pH-Gated photophysics of these compounds led to the development of pH-activated DNA cleavers which exhibit a dramatic increase in the ds:ss ratio at the lower pH of cancer cells. This family of DNA-photocleavers induced efficient cleavage of intracellular

DNA and lead to pronounced cytotoxicity to a variety of cancer cell lines upon photochemical activation.³³

Conveniently, the five-membered ring products have lower symmetry than the Bergman cyclizations products, and thus, one can use the *regioselectivity* of the nonsymmetric C1–C5 ring closure step as an alternative experimental probe for the remote substituent effects (Figure 8). The comparison of

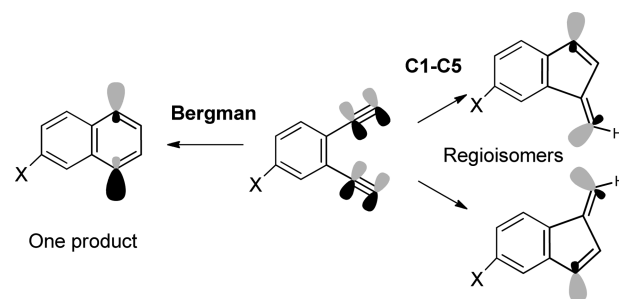


Figure 8. Comparison of regioselectivity for the Bergman and C1–C5 cycloaromatizations of eneidyne. Formation of regioisomers in the C1–C5 closure allows observation of remote substituent effects on the cycloaromatization barriers.

two alternative reactions of the same reactant is more straightforward than the comparison of rates for different reactants because it avoids the complications associated with differences in the reduction potentials and electron-transfer rates for eneidyne with different substituents and the known effect of accelerating charge introduction on reaction rates.^{34,35}

Because C1–C5 cyclization involves a crossing between orthogonal MOs in the same way (Figure 9 left) as the Bergman cyclization, this reaction also becomes highly sensitive to remote substitution upon electron injection.³⁶ The variations in the calculated activation energies exceed 20 kcal/mol, which suggests the possibility of dramatic variations in the cyclization rates. Figure 9 illustrates that the accelerating effect of donor substituents corresponds to classic reactant destabilization whereas the decelerating effect of acceptors stems from reactant stabilization.³⁷

In summary, the effects of remote substituent on regioselectivity of reductive C1–C5 cyclizations should provide experimental verification of MO-crossings between orthogonal orbitals as a new fundamental concept for the control of chemical reactivity. The comparison of *radical-anionic and dianionic* processes will reveal how the number of electrons involved in the crossings modulates communication between the electronic

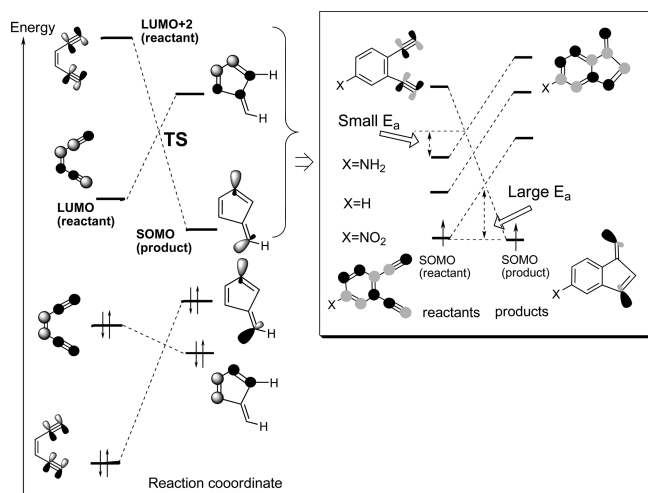


Figure 9. Left: Partial MO correlation diagram for radical-anionic C1–C5 cyclization of enediynes. Right: MO-crossing model of the role of remote substituents in defining the activation barrier for the radical anionic C1–C5 cyclization. Note that it only corresponds to the top part of the diagram shown on the left.

states during the cyclization process. Additionally, such substituent effects may resolve mechanistic ambiguities regarding the possible oxidation state of cyclizing species (*vide infra*).

COMPUTATIONAL DETAILS AND METHODS

Reaction energies and activation barriers were calculated at the M06-2x/6-31+G** level of theory using Gaussian-09 software.³⁸ M06-2x was used because it can describe cycloaromatization reactions with

sufficient accuracy.³⁹ The LanL2DZ basis set was used for calculations of Sn-containing species. Transition states were determined using the QST3 method. Frequency calculations were performed to confirm each stationary point as a minimum or a first-order saddle point. NBO analysis was used to analyze the electronic structures of reactants and transition states.⁴⁰ Electrostatic maps were processed by Molekel.⁴¹

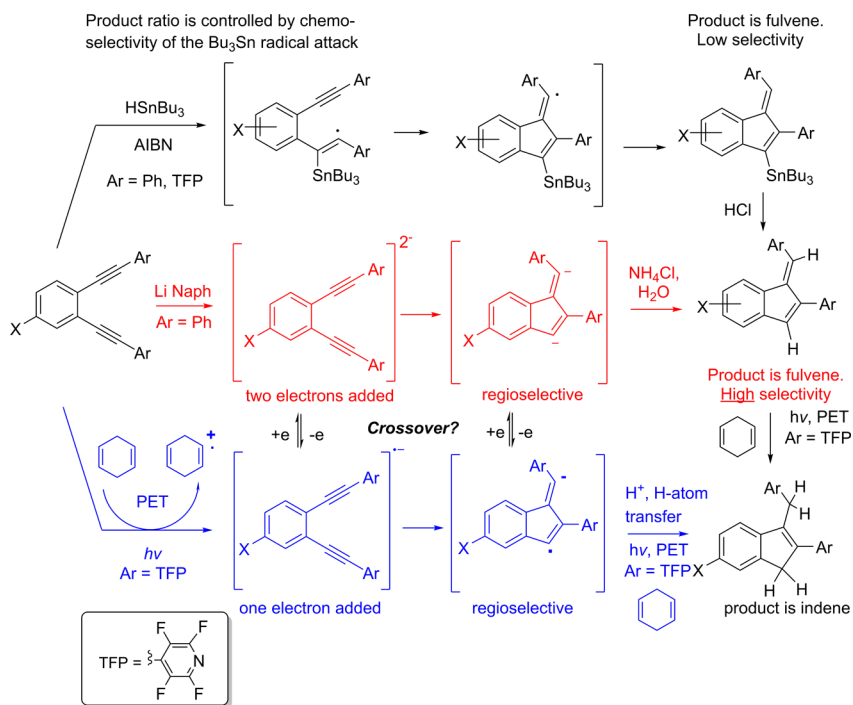
RESULTS AND DISCUSSION

Experimental Design. We investigated the regioselectivity of C1–C5 cyclization of enediynes under two sets of reducing conditions: lithium naphthalenide-promoted cyclizations of enediynes with terminal phenyl substituents and cyclization of bis-TFP-substituted enediynes promoted by photoinduced electron transfer (PET).

For the lithium naphthalenide reduction (the middle path in Scheme 1), the earlier work of Whitlock and co-workers²⁵ illustrated that two moles of the one-electron donor are needed. For the PET-cyclization in the bottom part of Scheme 1, an earlier work from our group also confirmed the intermediacy of at least two electron-transfer steps in the overall enediyne → fulvene → indene transformation.⁴² For reductive cyclizations, both regioisomers are produced from a common intermediate. In these reactions, the regioselectivity should be determined by the MO crossing-mediated effect of remote substitution on the cycloaromatization TSs.

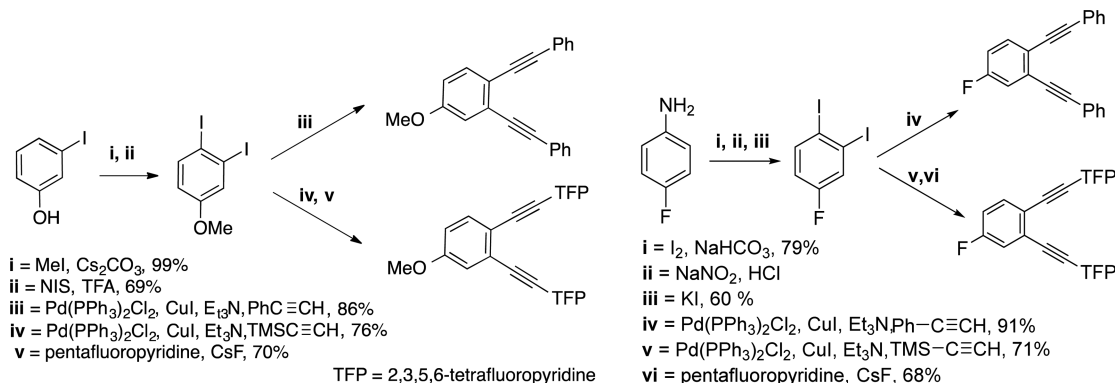
For comparison, we have also carried out Bu₃Sn-promoted radical cyclizations of the same substrates.⁴³ In the latter case, the two fulvene regioisomers are formed from different intermediates, each resulting from attack of the neutral radical species at one of the enediyne triple bonds (top of Scheme 1). This process was not expected to show significant regioselectivity. The Bu₃Sn-mediated reaction turned out to be a convenient

Scheme 1. Proposed Use of C1–C5 Cyclization of Benzannulated Enediynes as an Experimental Probe for the Role of Substituent Effects in Reductive Cycloaromatizations^a



^aThe three alternative ring closure modes provide different mechanistic information and regioselectivity. In each case, the enediyne reactants can form two fulvene regioisomers. See text for the discussion of contrasting expectations for the regioselectivity.

Scheme 2. Synthesis of Substituted Benzannelated Eneidyne

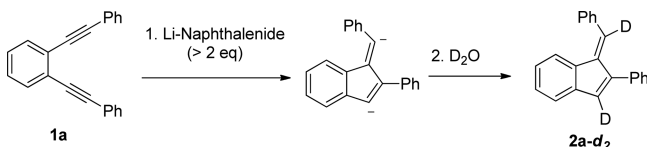


alternative way for the preparation of the minor products of these highly selective anionic cycloaromatizations.

Experimental Results. Synthesis of Eneidyne. Phenyl- and trimethylsilyl (TMS)-substituted eneidyne were synthesized via Sonogashira cross-coupling of the corresponding 3,4-diiodo-substituted benzenes (prepared as shown in Scheme 2 and discussed in the Supporting Information (SI)) with phenylacetylene and TMS acetylene, respectively. The substitution of the TMS moiety by the TFP group was performed via a one-pot deprotection–nucleophilic coupling procedure using pentafluoropyridine and cesium fluoride.⁴⁴

Eneidyne Cyclizations Induced by Lithium Naphthalenide. Whitlock and co-workers were the first to use lithium naphthalenide to achieve reductive cyclization of 1,2-diethynylphenylbenzene into the respective fulvene.²⁵ They also reported incorporation of two deuterium atoms upon quenching with D₂O as evidence that the cyclization proceeds via a dianion (Scheme 3). The intermediacy of a

Scheme 3. D₂O Quenching of the Lithium Naphthalenide-Mediated Cyclizations of Eneidyne Leads to Complete Deuterium Incorporation at Each of the Two Vinyl Carbons, Indicating the Intermediacy of a Dianion²⁵



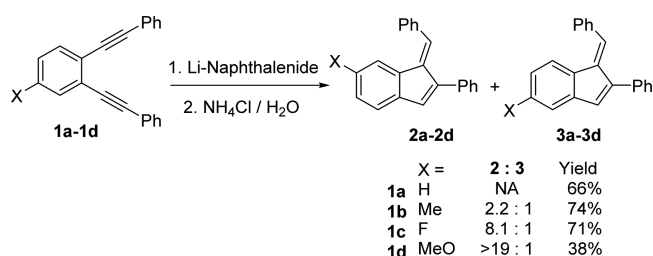
dianion is also consistent with the need for 2 equiv of the reducing agent for the reaction to proceed to completion. The didehydrofulvene dianion is stable toward further reduction and furnishes fulvene upon quenching with a proton source.⁴⁵

To our delight, not only were the cyclizations of eneidyne with a remote substituent at the benzene core regioselective, but the degree of selectivity depended on the substituent X at the aromatic core. The greatest selectivity (>19:1) was observed for X = OMe, whereas X = F and Me had shown lower selectivity (8:1 and 2:1, respectively) (Scheme 4).

Since lithium naphthalenide reduces most acceptor groups such as a nitro or an acyl group,⁴⁶ we were limited in the choice of substituents. For example, for X = Cl, the cyclization was accompanied by reductive dechlorination, leading to the formation of the unsubstituted fulvene 2a (Scheme 5). Even when the relative amount of lithium naphthalenide was reduced from 4 to 1 equiv, the dechlorinated eneidyne was formed in 64% yield as the only observed product. This result is not surprising considering the high reactivity of lithium naphthalenide—a strong reducing agent⁴⁷ with a reduction potential of −3.0 eV.^{48,49}

Effect of Terminal Substituents. In order to gain further understanding of electronic effects in the TS, we have investigated the regioselectivity of reductive eneidyne cyclizations in non-symmetric eneidyne where one of the terminal groups was changed from Ph to a different aromatic group.

Scheme 4. Experimentally Determined Products for the Dianionic C1–C5 Cyclization, Their Yields, and the Corresponding Ratios of Regioisomers



Scheme 5. Dianionic C1–C5 Cyclization of Eneidyne and Reductive Dechlorination Induced by Lithium Naphthalenide

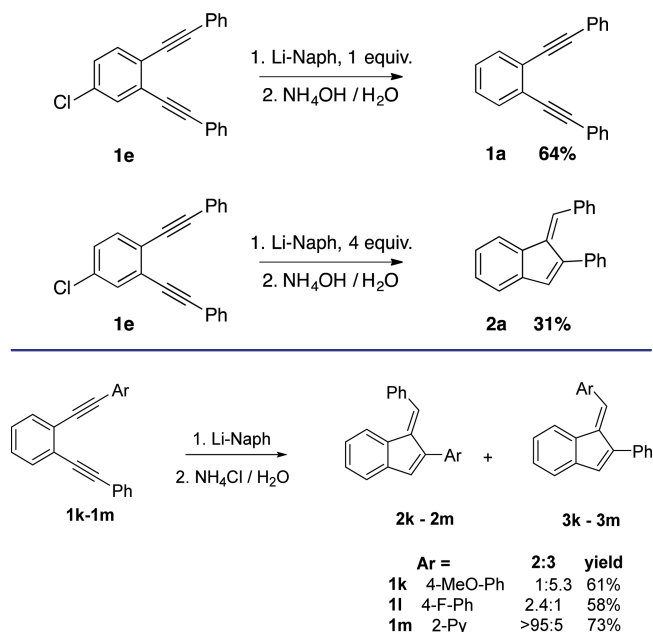


Figure 10. Cyclization of eneidyne 1k–1m with lithium naphthalenide.

Experimental results summarized in Figure 10 revealed an interesting reactivity pattern. Whereas the selectivity for the F-substituted substrate is relatively low (2.4:1 in favor of isomer 2l with F-Ph at the endocyclic position), the presence of the strong donor *p*-methoxy (OMe) group in 1k changes the observed selectivity in favor of the opposite isomer with the donor group at the exocyclic carbon. The acceptor Py group of 1m prefers an endocyclic position, forming a single fulvene regioisomer 2m.

PET-Promoted Reductive Cyclizations. Not surprisingly, the TFP moiety is unstable in the presence of lithium naphthalenide. Due to this high reactivity, the cyclizations of the TFP-substituted enediynes were studied under milder reducing conditions which utilized PET from 1,4-cyclohexadiene (1,4-CHD). We have shown earlier that this electron transfer is highly exothermic and fast.²⁶

The observed selectivity followed the same trends as above in the case of Li-mediated cyclizations of Ph-substituted enediynes (Scheme 6). This result reinforces the notion that the cyclizing species in the photoinduced cyclization of the TFP-enediynes is also a reduced form of enediyne (either a radical-anion or a dianion) and that similar MO crossings are involved in the control of regioselectivity via a one-electron reduction. Changing the Ph to a TFP group at the enediyne termini and the significant differences in reaction conditions had surprisingly small effects on cyclization regioselectivity in the cases of X = OMe and F. The relatively low regioselectivity for the cyclization of Me-substituted diphenyl enediyne **1b** decreased even further for the cyclization of analogous di-TFP enediyne **1f**. Interestingly, we have not observed reductive dechlorination (X = Cl → X = H) in the TFP-substituted enediynes under PET conditions.

Qualitatively, the effects for the Li- and PET-promoted cyclizations were expected to be similar because, the MO crossings in both the radical-anionic and the dianionic cycloaromatization reactions coincide with the TSs. As the result, p-donor substituents should control regioselectivity in a similar way. However, unlike the dianionic cyclizations, orbital crossings in radical-anionic cycloaromatizations involve MOs populated with one electron, and one could expect a weaker remote substituent effect. We will address this question below in the computational section of this work.

Photophysics. The rate of formation of OMe-substituted indenenes **2i/3i** in the photochemical cyclization was very slow compared to the other entries. To understand the reasons for this behavior,

Stern–Volmer analysis was performed on all TFP-substituted enediynes (discussed in detail in the SI).

Although the OMe derivative **1i** had the longest excitation lifetime (4.2 vs 1.5–2.6 ns), it also has the lowest driving force for the PET from 1,4-CHD in comparison to the other tested enediynes. The ~100-fold difference in the rate of electron transfer (10^8 vs 10^{10} M⁻¹ s⁻¹) explains the slower reaction with the OMe substrate. This example illustrates why it is easier to interpret substituent effects on selectivity than the effects on the overall reaction rates and yields in these systems.

Structure Determination. The structure of the major fulvene isomer for the F-substituted indene **4h** was unequivocally proven by X-ray crystallography (Figure 11). Interestingly, even in the crystal, 8% of the other regioisomer was still present co-crystallized together with 92% of the main component, **4a**, in the crystal packing.

The regioselectivity for the cyclization of other enediynes was determined by analyzing the structures of the two isomers with multi-nuclear 2D NMR spectroscopy and 1D NOESY experiments (see the SI). The separation of the isomeric indenenes derived from methyl-substituted enediyne proved to be difficult even with preparative HPLC. Because the ¹H NMR isomer ratio for this case was very close to 1:1, identification of the two isomers in this system has not been pursued.

The unambiguous assignment of the exo- and endocyclic vinylic protons in fulvenes can be accomplished using selective deuteration at one of the two vinylic positions, as described by us earlier using either the Bu₃SnH/DCl or Bu₃SnD/HCl combination of reagents (Scheme 7).^{43b} The exocyclic C–H in these fulvene structures is deshielded by ~0.4 ppm relative to the endocyclic C–H.

Further structural assignments were carried out by combining HSQC and HMBC analysis as analyzed in detail in the SI. The general trends for the fulvene isomers agreed well with the relative NMR values for similar structures published by Lautens and Wu.⁵⁰

Scheme 6. Experimentally Determined Products for the PET-C1–C5 Cyclization, Their Yields, and the Corresponding Ratio of Regioisomers

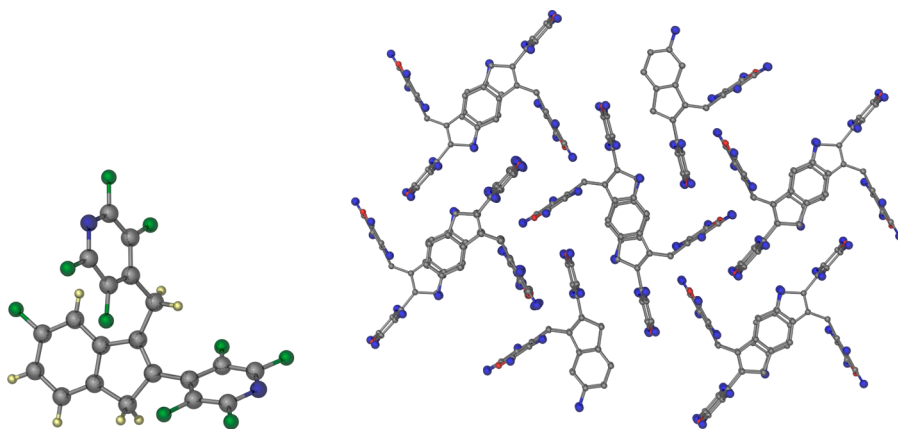
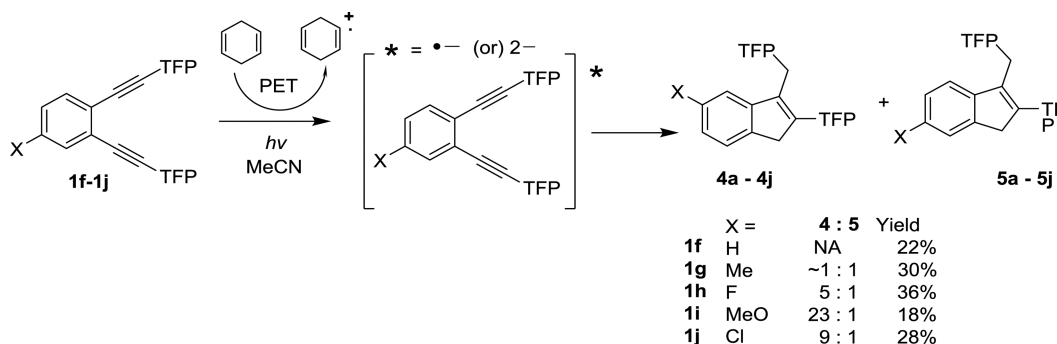


Figure 11. Left: X-ray crystal structure of F-substituted bis-TFP indene, **4h**, confirming the regioselectivity of the cyclization. C: gray; N: blue; F: green; H: small yellow. Right: Crystal packing of indene **4h**. Hydrogen and fluorine atoms are omitted for clarity in the right figure.

Scheme 7. Selective Deuteration Provides Access to Four Fulvene Isotopomers and Allows Unambiguous Assignment of NMR Signals for the Endo- and Exocyclic Vinyl Protons

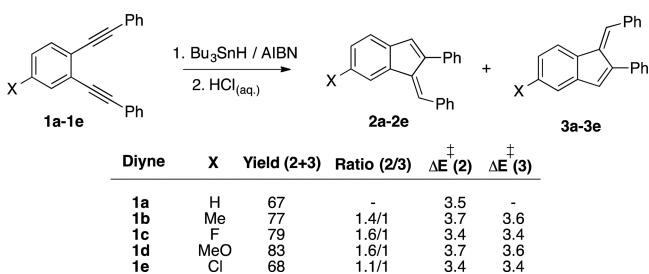
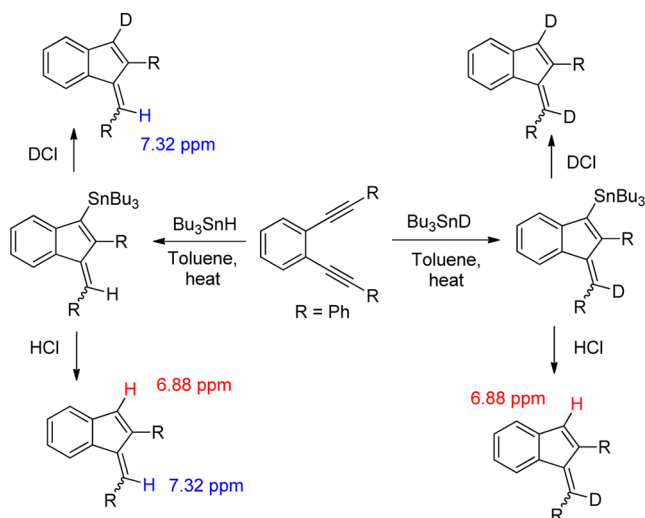


Figure 12. Summary of tributyltin hydride-promoted cyclization of enediynes. Transition-state energies for the cyclizations are given relative to the vinyl radicals produced upon tin addition to each triple bond and were calculated at the M06-2X/LanL2DZ/6-31G** level. The calculated energies of the initial tin addition products are within 0.5 kcal/mol of each other.

Tributyltin-Mediated Radical Cyclization of Eneidyne. Radical 5-*exo*-dig cyclizations of the phenyl-substituted enediynes were carried out using the tributyltin hydride/AIBN system (Figure 12).^{43,51} The advantage of this method is that the Bu₃Sn group can be removed by protic acids to afford the same fulvenes as in the Li-mediated cyclizations. Optimal conditions involved addition of a Bu₃SnH/AIBN mixture via syringe pump to the solution of enediyne in toluene under reflux, followed by proto-destannylation of the cyclized products with HCl (or AcOH for electron-rich and acid-sensitive OMe-substituted fulvene). In addition to the convenient conditions and the preparatively useful 70–80% yields, the radical reactions provide a greater amount of isomers corresponding to the minor products of the dianionic ring closures.

The observed 5-*exo* selectivity is consistent with the known preferences for the radical cyclizations of alkynes.⁵² The regioselectivity of these reactions is dependent on the initial chemoselectivity of the addition of tributyltin radical, rather than on orbital crossings. The ratios of products ranged from 1:1 to 1.5:1 indicating that both triple bonds have similar reactivity toward the intermolecular addition of the tin radical.⁵³

Radical cyclization was also expanded to include terminally substituted enediynes to further test selectivity in the absence of anionic MO crossings (Figure 13). Again, the ratio of products in these radical reactions is based solely on the chemoselectivity of addition to one of the two triple bonds instead of orbital crossing. Interestingly, even though the reaction produces essentially a 1:1 mixture of both isomers, the preference for the attack at the triple bond slightly increases in the order F > H > OMe.

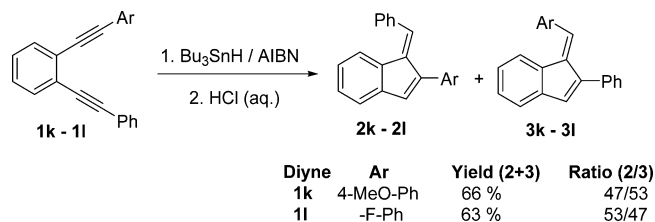


Figure 13. Bu₃SnH-promoted radical cyclization of terminally substituted enediynes.

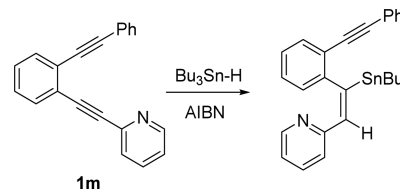


Figure 14. Reaction of tributyltin hydride with Py-substituted alkyne **1m** gave an acyclic product.

Unexpectedly, the reaction of nucleophilic tributyltin radical to 2-pyridyl enediyne **1m** is fully chemoselective but does not provide a cyclic product. Instead, the reaction proceeds via formal syn-addition at the Py-substituted alkyne (Figure 14). The stereochemistry was assigned on the basis of the 64 Hz value of the vicinal H–Sn coupling constant.⁵⁴ Although the regiochemistry of addition could not be determined unambiguously, the HMBC correlations are in a better agreement with the Sn attack at the carbon atom away from the pyridine (see the SI).

Computational Analysis of Reductive Cycloaromatizations. Analysis of computational data revealed a very interesting electronic reorganization that occurs along the reaction coordinate. The reasons for this electronic reorganization are two-fold: (a) delocalized π -anions are converted into a localized endocyclic vinyl anion and, to some extent, (b) the exocyclic π -system undergoes additional polarization toward the core with the concomitant increase in the aromatic cyclopentadienyl-anion character of the newly formed five-membered ring.

Interestingly, unlike the thermal TS and the anionic reactant and product, the core of the anionic TS is distinctly nonplanar. This nonplanarity assists in the negative charge delocalization by allowing the mixing of “in-plane” and “out-of-plane” orbitals at the MO crossing point (Figure 15). The single most dramatic change at the atomic level is the accumulation of ~ 0.3 electron at the endocyclic carbon that corresponds to the localized vinyl anion in the product.

Model for Substituent Effects in Reductive C1–C5 Cyclizations. Due to the observed negative charge accumulation patterns for the parent cycloaromatization, one can suggest a simple model to predict and rationalize substituent effect on the selectivity of ring closure. In this model, one would expect the introduction of acceptor groups at the para position relative to the endocyclic anionic carbon to have the largest stabilizing influence. An acceptor at the exocyclic anionic center is expected to have a lower impact. Donor substituents should have an opposite effect on regioselectivity via selective destabilization of the respective TSs (“Type D” products, Figure 16).

Computed Substituent Effects at Two Reductive Levels. We have initiated computational studies for testing the above model for the observed regiochemistry with the focus on the same selection of substituents that was compatible with the experimental conditions. The computational analysis paints a complicated picture which is different for Ph and TFP substrates at the different reduction stages (Figure 17).

For the radical-anionic cyclizations of Ph enediynes, all substituents favor formation of the Type A (“para”) product. The differences are larger (0.5–0.8 kcal) for the F- and OMe-substituted substrates, whose cyclizations were found the most selective experimentally. The methyl-substituted enediynes were not predicted to display significant regio-

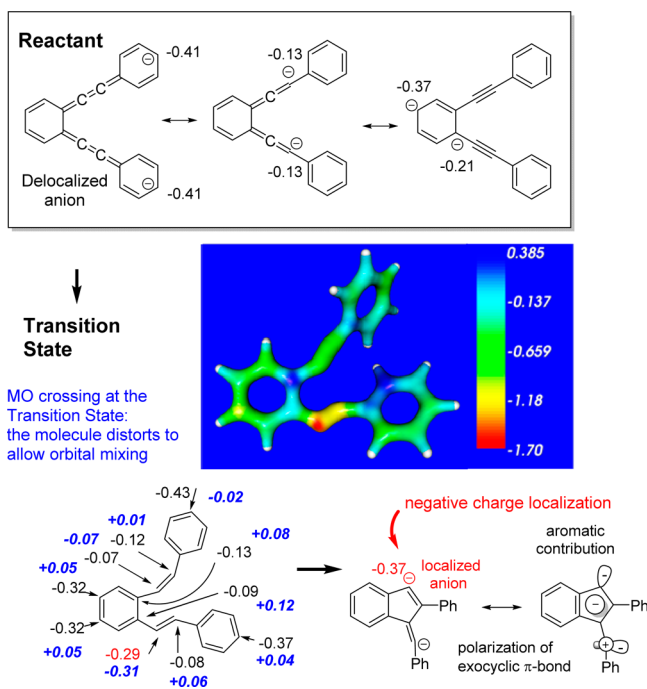


Figure 15. Evolution of electron density during cycloaromatization of delocalized enediyne dianion into partially localized benzofulvene dianion is illustrated using selected NBO charges in the reactant and product. Changes in charge in TS relative to the reactant are shown in blue bold italics. Negative and positive values indicate an increase and a decrease in electron density, respectively.

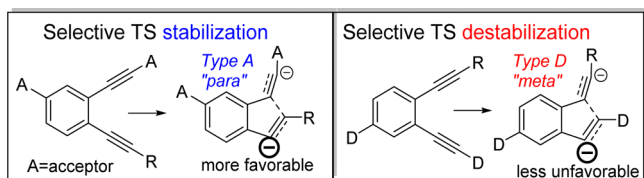


Figure 16. Expected substituent effects on the regioselectivity of anionic C1–C5 ring closure. Site with the largest accumulation of the negative charge in the TS (the endocyclic vinyl carbon of the fulvene moiety) is indicated with a larger negative charge sign.

selectivity in their reductive cyclization. This matches the experimentally observed ~1:1 ratio of products. The methyl group cannot act as a strong σ -acceptor and the C–C bond from the benzene ring to the methyl substituent is only weakly polar. These results agree with the experimental trends. In contrast, the computational data for the analogous TFP substrates show the opposite trend. According to the computational results, the terminal aromatic groups have a large effect on the reactions since they participate strongly in delocalization of the excessive electronic density. This effect is probably exaggerated in comparison to the experiments where solvent and counterion effects can strongly attenuate the importance of delocalization.

Computed energies for the dianionic cyclizations of Ph substrates, do not follow the experimental trend. For these substrates, computed selectivities for each substituent are very low. There are two possible explanations for the clear disagreement with the experiment: (1) a trivial one (the problems with the available theory) and (2) a more interesting one (the cyclizations occur at the radical-anionic stage and the second reduction occurs after the cyclization). The second scenario is reasonable because, after cyclization, the two nonbonding orbitals of the product are spatially separated, so the molecule should be less reluctant to accept one more negative charge. Because radical-anionic cyclizations are endothermic, fast reduction of the cyclic product may play a significant role in driving the process forward to the formation of cyclic species. Note that reactions of Ph substrates

proceed under the dissolving metal conditions where concentration of electrons is always relatively large and, thus, the transiently formed cyclic species can be trapped.

The trends for the cyclizations of mono- and di-reduced species are reversed for the TFP-enediynes. Whereas the calculated trends for the radical-anionic pathways do not follow the experimental selectivities, the calculated trends for dianionic cyclizations do, supporting a different reductive state for the cyclizing species relative to the case of Ph-enediynes. One can rationalize the difference by remembering that reaction conditions for the two reductive processes are drastically different. For the photochemical processes, the transiently formed cyclic product is unlikely to receive the second electron in time to prevent the retro-C1–C5 ring opening.⁵⁵ Thus, the radical-anionic pathway remains unproductive and, only the second electron is transferred,⁵⁶ the cyclization is possible. This scenario is consistent with the significant exothermicity (=effective irreversibility) of the dianionic cycloaromatization.

Overall, the computed selectivities agree with the experimental selectivities if Ph substrates cyclize at the radical-anionic stage whereas the ring closure of TFP substrates only happens upon the formation of a dianion. In this scenario, the similarity between observed substituent effects on the Li-promoted cyclizations of Ph-enediynes and PET-promoted cyclization of TFP-enediynes seems fortuitous. One can rationalize this intriguing situation by suggesting that additional charge injection is needed for forcing the more stabilized and less reactive TFP substrates to undergo the cyclization path. This suggestion seems reasonable, but it is also clear that these processes pose a considerable challenge for theory. Most likely, inclusion of explicit Li counterions as well as the solvation effects is necessary to model such systems confidently.

In summary, although experimental trends are clear and large substituent effects are observed, their computational description is so far problematic. Such reductive cycloaromatization reactions clearly present a challenge to the DFT theory available for these relatively large systems. Effects of solvation and introduction of explicit counterions may be necessary, especially for the highly charged dianionic species.

CONCLUSIONS

Transition states of the reactions that involve a bond-breaking event in the direct vicinity of an orthogonal π -system activate orbital crossings between the two orthogonal orbital systems. When at least one of the crossing MO levels is neither completely empty nor completely occupied, such crossings correspond to intramolecular electron transfer between the two orthogonal systems and can be used to effectively control activation barriers and reaction energies.

The present work highlighted the effect of MO crossings on the regioselectivity of C1–C5 cycloaromatization reaction of benzannelated enediynes. We have shown experimentally that reductive C1–C5 cyclization reactions of substituted benzannelated enediynes are regioselective, especially in the presence of anion-stabilizing donor groups.

The regioselectivity of the C1–C5 cycloaromatization reaction of benzannelated enediynes is efficiently controlled by remote substitution.

From a practical point of view, we had found substitution patterns capable of controlling the regioselectivity and efficiency of reductive C1–C5 cyclizations of enediynes. The increased chemical yields and amplified regioselectivity confirm the increased importance of remote substitution and orbital crossings. This work, for the first time, illustrates a new paradigm for control of reaction rates based on electronic communication between orthogonal orbitals activated via electron injection. Studies of analogous effects promoted by hole injection are underway.

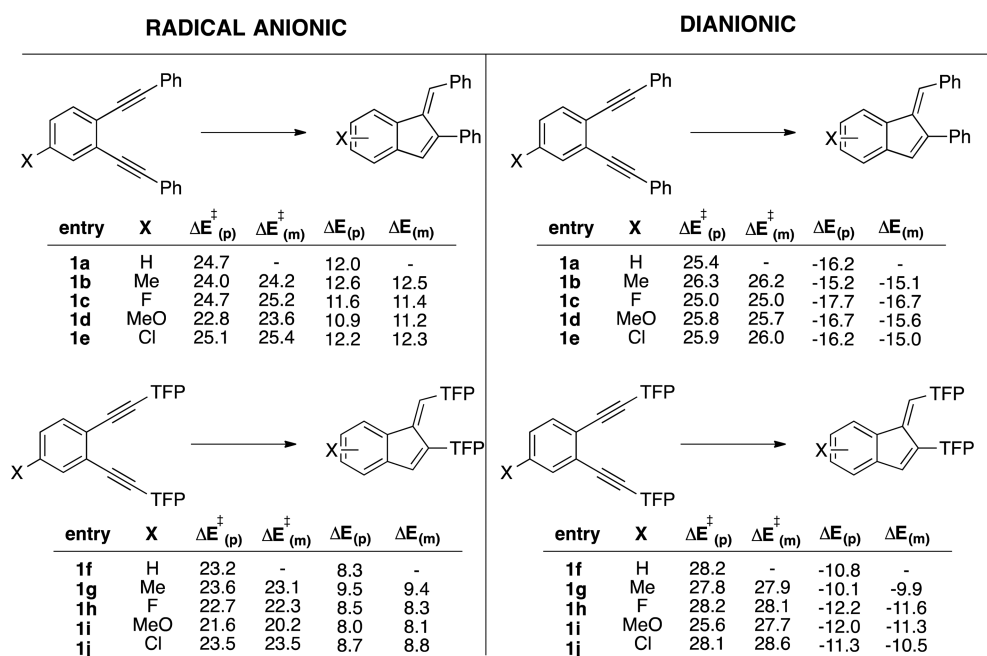


Figure 17. Calculated activation and reaction energies (kcal/mol) at the M06-2X/6-31+G(d,p) level for radical anionic (left) and dianionic (right) cyclizations. Definitions for “meta” and “para” regioselectivities for the ring closure are given in Figure 16. Additionally, a graphical representation of these results is given in the computational analysis part of the SI.

The observed experimental data can only be reconciled with the computational results if cyclizations at the different reduction state are suggested for the Ph- and TFP-substituted enediyne. The experimental selectivities for Ph-enediynes are consistent with the calculated barriers for the radical anionic ring closures. In contrast, the observed selectivities of TFP-enediynes cyclizations are consistent with the computed barriers for the dianionic pathways, suggesting the stabilized anionic species are more reluctant to undergo cycloaromatization.

■ ASSOCIATED CONTENT

📄 Supporting Information

The Supporting Information is available free of charge on the ACS Publications website at DOI: 10.1021/jacs.6b08540.

Experimental details, NMR spectra and full characterization data for all new compounds, coordinates for all computational results, crystallography data, UV spectra, and Stern–Volmer analysis details, as well as analysis of 2D NMR data (PDF)

X-ray crystallographic data for C₂₀H₇F₉N₂ (CIF)

■ AUTHOR INFORMATION

Corresponding Author

*alabugin@chem.fsu.edu

Present Address

†Department of Chemistry, University of California, Davis.

ORCID

Igor V. Alabugin: 0000-0001-9289-3819

Notes

The authors declare no competing financial interest.

■ ACKNOWLEDGMENTS

I.A. is grateful to the National Science Foundation (CHE-1465142) for support of this research project. We also

acknowledge help and advice from Michael Shatruk, Flynt Goodson, and Sourav Saha.

■ REFERENCES

- Milián-Medina, B.; Gierschner, J. *WIREs Comput. Mol. Sci.* **2012**, *2*, 513.
- Alabugin, I. V.; Gilmore, K. M.; Peterson, P. W. *WIREs Comput. Mol. Sci.* **2011**, *1*, 109. Cramer, C. J. *J. Mol. Struct.: THEOCHEM* **1996**, *370*, 135.
- Deslongchamps, P. *Stereoelectronic Effects in Organic Chemistry*; Pergamon Press: Oxford, England, 1983. Kirby, A. *J. Stereoelectronic Effects*; Oxford University Press: Oxford, England, 1996. Juaristi, E.; Cuevas, G. *Acc. Chem. Res.* **2007**, *40*, 961. Alabugin, I. V. *Stereoelectronic Effects: The Bridge between Structure and Reactivity*; John Wiley & Sons Ltd, Chichester, UK, 2016.
- Birtles, R. H.; Hampson, G. C. *J. Chem. Soc.* **1937**, 10.
- (a) Jones, R. R.; Bergman, R. G. *J. Am. Chem. Soc.* **1972**, *94*, 660. (b) Bergman, R. G. *Acc. Chem. Res.* **1973**, *6*, 25.
- Galbraith, J. M.; Schreiner, P. v. R.; Harris, N.; Wei, W.; Wittkopp, A.; Shaik, S. *Chem. - Eur. J.* **2000**, *6*, 1446.
- Choy, N.; Kim, C. S.; Ballester, C.; Artigas, L.; Diez, C.; Lichtenberger, F.; Shapiro, L.; Russell, K. C. *Tetrahedron Lett.* **2000**, *41*, 6955. The correlation of the reaction rate with the Hammett σ_m value revealed a low sensitivity to substituents ($\rho = 0.654$). The Swain–Lupton model yielded a field parameter (0.662) larger than the resonance parameter (0.227), indicating that conjugative effects in the out-of-plane π -system are of lesser importance than field effects.
- Alabugin, I. V.; Manoharan, M.; Kovalenko, S. V. *Org. Lett.* **2002**, *4*, 1119. Zeidan, T.; Kovalenko, S. V.; Manoharan, M.; Alabugin, I. V. *J. Org. Chem.* **2006**, *71*, 962. Zeidan, T.; Manoharan, M.; Alabugin, I. V. *J. Org. Chem.* **2006**, *71*, 954.
- For representative examples of a variety of cycloaromatization reactions, see: (a) Nagata, R.; Yamanaka, H.; Okazaki, E.; Saito, I. *Tetrahedron Lett.* **1989**, *30*, 4995. Myers, A. G.; Dragovich, P. S.; Kuo, E. Y. *J. Am. Chem. Soc.* **1992**, *114*, 9369. (b) Nakatani, K.; Isoe, S.; Maekawa, S.; Saito, I. *Tetrahedron Lett.* **1994**, *35*, 605. Sullivan, R. W.; Coghlan, V. M.; Munk, S. A.; Reed, M. W.; Moore, H. W. *J. Org. Chem.* **1994**, *59*, 2276. (c) Toda, F.; Tanaka, K.; Sano, I.; Isozaki, T. *Angew. Chem., Int. Ed. Engl.* **1994**, *33*, 1757. (d) Nicolaou, K. C.; Skokotas, G.;

- Maligres, P.; Zuccarello, G.; Schweiger, E. J.; Tushima, K.; Wendeborn, S. *Angew. Chem., Int. Ed. Engl.* **1989**, *28*, 1272. (e) Engels, B.; Lennartz, C.; Hanrath, M.; Schmittel, M.; Strittmatter, M. *Angew. Chem.* **1998**, *110*, 2067. (f) Schmittel, M.; Steffen, J. P.; Angel, M. A. W.; Engels, B.; Lennartz, C.; Hanrath, M. *Angew. Chem., Int. Ed.* **1998**, *37*, 1562. (g) Schmittel, M.; Rodriguez, D.; Steffen, J. P. *Angew. Chem., Int. Ed.* **2000**, *39*, 2152. (h) Kawatkar, S. P.; Schreiner, P. R. *Org. Lett.* **2002**, *4*, 3643. (i) Mondal, S.; Mitra, T.; Mukherjee, R.; Addy, P. S.; Basak, A. *Synlett* **2012**, *23*, 2582. (j) Das, J.; Das, E.; Jana, S.; Addy, P. S.; Anoop, A.; Basak, A. *J. Org. Chem.* **2016**, *81*, 450. Review: (k) Mohamed, R. K.; Peterson, P. W.; Alabugin, I. V. *Chem. Rev.* **2013**, *113*, 7089. Radical/ionic dichotomy: (l) Peterson, P. W.; Mohamed, R. K.; Alabugin, I. V. *Eur. J. Org. Chem.* **2013**, *2013*, 2505.
- (10) (a) *Enediyne Antibiotics as Antitumor Agents*; Borgers, D. B., Doyle, T. E., Eds.; Marcel Dekker: New York, 1995. (b) *Neocarzinostatin: The Past, Present, and Future of an Anticancer Drug*; Maeda, H., Edo, K., Ishida, N., Eds.; Springer: New York, 1997.
- (11) Wu, M.; Stoermer, D.; Tullius, T.; Townsend, C. A. *J. Am. Chem. Soc.* **2000**, *122*, 12884.
- (12) Bowles, D. M.; Palmer, G. J.; Landis, C. A.; Scott, J. L.; Anthony, J. E. *Tetrahedron* **2001**, *57*, 3753. Bowles, D. M.; Anthony, J. E. *Org. Lett.* **2000**, *2*, 85.
- (13) Chen, X.; Tolbert, L. M.; Hess, D. W.; Henderson, C. *Macromolecules* **2001**, *34*, 4104. Shah, H. V.; Babb, D. A.; Smith, D. W., Jr. *Polymer* **2000**, *41*, 4415. John, J. A.; Tour, J. M. *J. Am. Chem. Soc.* **1994**, *116*, 5011.
- (14) Alabugin, I. V.; Manoharan, M. *J. Am. Chem. Soc.* **2003**, *125*, 4495.
- (15) The ability of fine-tuning of relative energies of two non-orthogonal but still pseudo-independent orbital systems has been a basis of creative photophysical designs. For examples, see: Zuccherro, A. J.; McGrier, P. L.; Bunz, U. H. F. *Acc. Chem. Res.* **2010**, *43*, 397. McGrier, P. L.; Solntsev, K. M.; Miao, S.; Tolbert, L. M.; Miranda, O. R.; Rotello, V. M.; Bunz, U. H. F. *Chem. - Eur. J.* **2008**, *14*, 4503. Wilson, J. N.; Bunz, U. H. F. *J. Am. Chem. Soc.* **2005**, *127*, 4124.
- (16) The term "MO crossings" used in this paper is analogous in meaning to "state crossings" used in photochemical literature.
- (17) Reed, A. E.; Curtiss, L. A.; Weinhold, F. *Chem. Rev.* **1988**, *88*, 899.
- (18) For the role of energy gap on the acceptor ability of σ -bonds, see: Alabugin, I. V.; Zeidan, T. A. *J. Am. Chem. Soc.* **2002**, *124*, 3175–3185.
- (19) For an application of this electronic phenomenon to alkyne cyclo-additions, see: Gold, B.; Shevchenko, N.; Bonus, N.; Dudley, G. B.; Alabugin, I. V. *J. Org. Chem.* **2012**, *77*, 75. Gold, B.; Dudley, G. B.; Alabugin, I. V. *J. Am. Chem. Soc.* **2013**, *135*, 1558. Synopsis: Alabugin, I. V.; Gold, B. *J. Org. Chem.* **2013**, *78*, 7777.
- (20) The "unreactive" out-of-plane π -system still plays an important role by providing electronic stabilization to the product. For an in-depth discussion of the contrasting role of the two orthogonal π -systems, see: Alabugin, I. V.; Breiner, B.; Manoharan, M. *Adv. Phys. Org. Chem.* **2007**, *42*, 1–35. See also: Alabugin, I. V.; Manoharan, M. *J. Phys. Chem. A* **2003**, *107*, 3363.
- (21) Selected recent examples: (a) Das, A.; Ghosh, I.; Konig, B. *Chem. Commun.* **2016**, *52*, 8695. (b) Ghosh, I.; Konig, B. *Angew. Chem., Int. Ed.* **2016**, *55*, 7676. (c) Ghosh, I.; Marzo, L.; Das, A.; Shaikh, R.; Konig, B. *Acc. Chem. Res.* **2016**, *49*, 1566. (d) Meyer, A. U.; Slanina, T.; Yao, C.-J.; Konig, B. *ACS Catal.* **2016**, *6*, 369.
- (22) Hoffmann, R.; Woodward, R. B. *Acc. Chem. Res.* **1968**, *1*, 17.
- (23) For "SOMO–HOMO level conversion" where SOMO is lower than the HOMO, see: (a) Gryn'ova, G.; Marshall, D. L.; Blanksby, S. J.; Coote, M. L. *Nat. Chem.* **2013**, *5*, 474. (b) Ishiguro, K.; Kamekura, Y.; Sawaki, Y. *Mol. Cryst. Liq. Cryst. Sci. Technol., Sect. A* **1993**, *233*, 113. (c) Kusamoto, T.; Kume, S.; Nishihara, H. *J. Am. Chem. Soc.* **2008**, *130*, 13844. (d) Kobayashi, Y.; Yoshioka, M.; Saigo, K.; Hashizume, D.; Ogura, T. *J. Am. Chem. Soc.* **2009**, *131*, 9995. (e) Sugawara, T.; Komatsu, H.; Suzuki, K. *Chem. Soc. Rev.* **2011**, *40*, 3105.
- (24) Prall, M.; Wittkopp, A.; Schreiner, P. R. *J. Phys. Chem. A* **2001**, *105*, 9265. Vavilala, C.; Byrne, N.; Kraml, C. M.; Ho, D. M.; Pascal, R. A. *J. Am. Chem. Soc.* **2008**, *130*, 13549.
- (25) Whitlock, H. W., Jr.; Sandvick, P. E.; Overman, L. E.; Reichardt, P. B. *J. Org. Chem.* **1969**, *34*, 879.
- (26) Alabugin, I. V.; Kovalenko, S. V. *J. Am. Chem. Soc.* **2002**, *124*, 9052.
- (27) Kovalenko, S. V.; Alabugin, I. V. *Chem. Commun.* **2005**, 1444.
- (28) Yang, W.-Y.; Breiner, B.; Kovalenko, S. V.; Ben, C.; Singh, M.; LeGrand, S. N.; Sang, A. Q.-X.; Strouse, G. F.; Copland, J. A.; Alabugin, I. V. *J. Am. Chem. Soc.* **2009**, *131*, 11458.
- (29) Elmroth, K.; Nygren, J.; Martensson, S.; Ismail, I. H.; Hammarsten, O. *DNA Repair* **2003**, *2*, 363.
- (30) Yang, W.-Y.; Roy, S.; Phrathep, B.; Kenworthy, R.; Rengert, Z.; Zorio, D. A. R.; Alabugin, I. V. *J. Med. Chem.* **2011**, *54*, 8501. For further correlations between structure and DNA-cleaving activity, see: Kaya, K.; Roy, S.; Nogues, J. C.; Rojas, J. C.; Sokolik, Z.; Zorio, D. A. R.; Alabugin, I. V. *J. Med. Chem.* **2016**, *59*, 8634.
- (31) Breiner, B.; Schlatterer, J. C.; Kovalenko, S. V.; Greenbaum, N. L.; Alabugin, I. V. *Angew. Chem., Int. Ed.* **2006**, *45*, 3666.
- (32) Breiner, B.; Schlatterer, J. C.; Alabugin, I. V.; Kovalenko, S. V.; Greenbaum, N. L. *Proc. Natl. Acad. Sci. U. S. A.* **2007**, *104*, 13016.
- (33) Review: Breiner, B.; Kaya, K.; Roy, S.; Yang, W.-Y.; Alabugin, I. V. *Org. Biomol. Chem.* **2012**, *10*, 3974–3987.
- (34) VB analysis: Shaik, S.; Shurki, A. *Angew. Chem., Int. Ed.* **1999**, *38*, 586.
- (35) (a) Bellville, D. J.; Wirth, D. D.; Bauld, N. L. *J. Am. Chem. Soc.* **1981**, *103*, 718. (b) Bellville, D. J.; Bauld, N. L. *J. Am. Chem. Soc.* **1982**, *104*, 2665. (c) Pabon, R. A.; Bellville, D. J.; Bauld, N. L. *J. Am. Chem. Soc.* **1983**, *105*, 5158. (d) Bernardi, F.; Bottoni, A.; Olivucci, M.; Venturini, A.; Robb, M. A. *J. Chem. Soc., Faraday Trans.* **1994**, *90*, 1617. (e) Jungwirth, P.; Bally, T. *J. Am. Chem. Soc.* **1993**, *115*, 5783.
- (36) Alabugin, I. V.; Manoharan, M. *J. Am. Chem. Soc.* **2003**, *125*, 4495.
- (37) In benzannelated enediynes, the MO crossing between the two orthogonal π -arrays has an additional role since it transforms an anti-aromatic π -anion into a localized σ -anion. During this change, an anti-aromatic reactant stabilizes itself by sending an in-plane electron to an out-of plane orbital and regaining aromaticity.
- (38) Frisch, M. J.; Trucks, G. W.; Schlegel, H. B.; Scuseria, G. E.; Robb, M. A.; Cheeseman, J. R.; Montgomery, J. A., Jr.; Vreven, T.; Kudin, K. N.; Burant, J. C.; Millam, J. M.; Iyengar, S. S.; Tomasi, J.; Barone, V.; Mennucci, B.; Cossi, M.; Scalmani, G.; Rega, N.; Petersson, G. A.; Nakatsuji, H.; Hada, M.; Ehara, M.; Toyota, K.; Fukuda, R.; Hasegawa, J.; Ishida, M.; Nakajima, T.; Honda, Y.; Kitao, O.; Nakai, H.; Klene, M.; Li, X.; Knox, J. E.; Hratchian, H. P.; Cross, J. B.; Bakken, V.; Adamo, C.; Jaramillo, J.; Gomperts, R.; Stratmann, R. E.; Yazyev, O.; Austin, A. J.; Cammi, R.; Pomelli, C.; Ochterski, J. W.; Ayala, P. Y.; Morokuma, K.; Voth, G. A.; Salvador, P.; Dannenberg, J. J.; Zakrzewski, V. G.; Dapprich, S.; Daniels, A. D.; Strain, M. C.; Farkas, O.; Malick, D. K.; Rabuck, A. D.; Raghavachari, K.; Foresman, J. B.; Ortiz, J. V.; Cui, Q.; Baboul, A. G.; Clifford, S.; Cioslowski, J.; Stefanov, B. B.; Liu, G.; Liashenko, A.; Piskorz, P.; Komaromi, I.; Martin, R. L.; Fox, D. J.; Keith, T.; Al-Laham, M. A.; Peng, C. Y.; Nanayakkara, A.; Challacombe, M.; Gill, P. M. W.; Johnson, B.; Chen, W.; Wong, M. W.; Gonzalez, C.; Pople, J. A. *Gaussian 03*, Revision C.02; Gaussian, Inc., Wallingford, CT, 2004.
- (39) (a) Mohamed, R. K.; Mondal, S.; Jorner, K.; Faria Delgado, T.; Lobodin, V. V.; Ottosson, H.; Alabugin, I. V. *J. Am. Chem. Soc.* **2015**, *137*, 15441. (b) Hoyer, T. R.; Baire, B.; Niu, D.; Willoughby, P. H.; Woods, B. P. *Nature* **2012**, *490*, 208.
- (40) Glendening, E. D.; Badenhop, J. K.; Reed, A. E.; Carpenter, J. E.; Bohmann, J. A.; Morales, C. M.; Weinhold, F. *NBO 5.0*; Theoretical Chemistry Institute, University of Wisconsin, Madison, WI, 2001.
- (41) Varetto, U. *MOLEKEL 4.3*; Swiss National Supercomputing Centre, Lugano, Switzerland.
- (42) Alabugin, I. V.; Kovalenko, S. V. *J. Am. Chem. Soc.* **2002**, *124*, 9052.

(43) (a) Kovalenko, S. V.; Peabody, S.; Manoharan, M.; Clark, R. J.; Alabugin, I. V. *Org. Lett.* **2004**, *6*, 2457. (b) Peabody, S.; Breiner, B.; Kovalenko, S. V.; Patil, S.; Alabugin, I. V. *Org. Biomol. Chem.* **2005**, *3*, 218.

(44) Artamkina, G. A.; Kovalenko, S. V.; Beletskaya, I. P.; Reutov, O. A. *Russ. J. Org. Chem.* **1990**, *26*, 225.

(45) If an excess of reducing agent was still present at the end of reaction, it was essential to carry out the quenching step quickly, i.e., with ammonium chloride and crushed ice. When a less reactive source of protons was used, such as cold methanol, the formation of over-reduced (indene) products was observed, suggesting that residual lithium remained while the fulvene dianion was protonated to give the neutral fulvene molecule, susceptible to the further reduction.

(46) (a) Zhang, H.; Karasawa, T.; Yamada, H.; Wakamiya, A.; Yamaguchi, S. *Org. Lett.* **2009**, *11*, 3076. (b) Yamaguchi, S.; Xu, C.; Tamao, K. J. *J. Am. Chem. Soc.* **2003**, *125*, 13662. (c) Xu, C.; Wakamiya, A.; Yamaguchi, S. *J. Am. Chem. Soc.* **2005**, *127*, 1638. (d) Xu, C.; Wakamiya, A.; Yamaguchi, S. *Org. Lett.* **2004**, *6*, 3707.

(47) Whitlock, H. W., Jr.; Sandvick, P. E.; Overman, L. E.; Reichardt, P. B. *J. Org. Chem.* **1969**, *34*, 879.

(48) Rele, S.; Talukdar, S.; Banerji, A.; Chattopadhyay, S. *J. Org. Chem.* **2001**, *66*, 2990. Lithium naphthalenide is reactive not only toward aryl chlorides but also toward a variety of functionalities. Geminal dihalides: Ashby, E. C.; Deshpande, A. K. *J. Org. Chem.* **1995**, *60*, 4530. Benzyl ethers: Liu, H.-J.; Yip, J.; Shia, K.-S. *Tetrahedron Lett.* **1997**, *38*, 2253. α,β -Epoxy ketones: Jankowska, R.; Mhehe, G. L.; Liu, H.-J. *Chem. Commun.* **1999**, *16*, 1581. α -Cyano ketones: Liu, H.-J.; Zhu, J.-L.; Shia, K.-S. *Tetrahedron Lett.* **1998**, *39*, 4183.

(49) Interestingly, this experimental observation is consistent with the spontaneous loss of chloride anion observed during DFT geometry optimization of **1n** at B3LYP/6-31G***, but not for B3LYP/6-31+G** and M05-2X/6-31+G** levels of theory. The terminal phenyl rings stabilized the anions sufficiently that barrierless dechlorination did not occur *in silico*. The optimized geometry of the radical anion of **1e** did not indicate the loss of chloride anion in gas- or solvent-phase calculations.

(50) (a) Bryan, C. S.; Lautens, M. *Org. Lett.* **2010**, *12*, 2754. (b) Ye, S.; Wu, J. *Org. Lett.* **2011**, *13*, 5980.

(51) For an earlier report of radical-mediated cyclization of enediyne, see: Koenig, B.; Pitsch, W.; Klein, M.; Vasold, R.; Prall, M.; Schreiner, P. R. *J. Org. Chem.* **2001**, *66*, 1742.

(52) Rules for anionic and radical alkyne cyclizations: Alabugin, I.; Gilmore, K.; Manoharan, M. *J. Am. Chem. Soc.* **2011**, *133*, 12608. Alabugin, I. V.; Gilmore, K. *Chem. Commun.* **2013**, *49*, 11246. Review: Gilmore, K.; Alabugin, I. V. *Chem. Rev.* **2011**, *111*, 6513. Note that the alternative 5-*endo*-dig cyclization in these systems are expected to be slow: Alabugin, I. V.; Timokhin, V. I.; Abrams, J. N.; Manoharan, M.; Ghiviriga, I.; Abrams, R. *J. Am. Chem. Soc.* **2008**, *130*, 10984. Alabugin, I. V.; Manoharan, M. *J. Am. Chem. Soc.* **2005**, *127*, 9534.

(53) Note, however, that this feature does not always lead to low selectivity. Highly selective radical cyclizations can be designed in multifunctional systems where initial selectivity of radical attack is low:

(a) Alabugin, I. V.; Gilmore, K.; Patil, S.; Manoharan, M.; Kovalenko, S. V.; Clark, R. J.; Ghiviriga, I. *J. Am. Chem. Soc.* **2008**, *130*, 11535.

(b) Mondal, S.; Mohamed, R. K.; Manoharan, M.; Phan, H.; Alabugin, I. V. *Org. Lett.* **2013**, *15*, 5650. (c) Mondal, S.; Gold, B.; Mohamed, R. K.; Alabugin, I. V. *Chem. - Eur. J.* **2014**, *20*, 8664. (d) Mondal, S.; Gold, B.; Mohamed, R.; Phan, H.; Alabugin, I. V. *J. Org. Chem.* **2014**, *79*, 7491. (e) Mohamed, R. K.; Mondal, S.; Gold, B.; Evoniuk, C. J.; Banerjee, T.; Hanson, K.; Alabugin, I. V. *J. Am. Chem. Soc.* **2015**, *137*, 6335. (h) Pati, K.; Gomes, G. P.; Harris, T.; Hughes, A.; Phan, H.; Banerjee, T.; Hanson, K.; Alabugin, I. V. *J. Am. Chem. Soc.* **2015**, *137*, 1165. (i) Evoniuk, C. J.; Ly, M.; Alabugin, I. V. *Chem. Commun.* **2015**, *51*, 12831. (k) Pati, K.; Michas, C.; Allenger, D.; Piskun, I.; Coutros, P. S.; Gomes, G. P.; Alabugin, I. V. *J. Org. Chem.* **2015**, *80*, 11706. (l) Mohamed, R. K.; Mondal, S.; Guerrero, J. V.; Eaton, T. M.; Albrecht-Schmitt, T. E.; Shatruck, M.; Alabugin, I. V. *Angew. Chem., Int. Ed.* **2016**, *55*, 12054.

(54) For *cis*-Sn–H couplings, *J* values range from 60 to 70 Hz, whereas *trans* geometries display *J* values from 120 to 130 Hz: (a) Mitchell, T. N.; Podesta, J. C.; Ayala, A.; Chopra, A. B. *Magn. Reson. Chem.* **1988**, *26*, 497. (b) Leusink, A. J.; Budding, H. A.; Marsman, J. W. *J. Organomet. Chem.* **1967**, *9*, 285.

(55) Of course, protonation of the cyclic radical-anion by the radical-cation of the donor may provide another possible trapping pathway. It is not clear, at this point, when this process may occur.

(56) The presence of the two powerful TFP acceptors in the molecule seems to be essential for this process to occur.